6.5 CLOUD-TO-GROUND LIGHTNING WARNINGS USING TOTAL LIGHTNING MAPPING AND ELECTRIC FIELD MILL OBSERVATIONS

Martin J. Murphy*, Ronald L. Holle, Nicholas W.S. Demetriades
Vaisala Inc.
Tucson, AZ

1. Introduction

Automated lightning warning systems are a critical component of many day-to-day operations. This is particularly true of airports but also applies in some industrial applications, such as mining and the manufacture, testing, and handling of explosives and weapons. Many automated lightning warning systems use a combination of lightning detection information and one or more electric field mills (EFMs). In previous studies (e.g. Murphy and Holle, 2006), we have analyzed the capability of various lightning detection systems to provide warning prior to the first cloud-to-ground (CG) lightning flash within an Area Of Concern (AOC) around a given point or facility requiring lightning safety information. The lack of continuously recorded EFM data was the primary hindrance to including EFMs as part of those previous studies. The purpose of this paper is to remedy that problem, at least for one particular location in the world where continuous EFM data are available.

Unlike lightning detection systems, which respond to fast transients in the electromagnetic field and/or optical signals generated by lightning, EFMs detect the electrostatic field and relatively slow changes in that field. They detect the presence of charge separation and net charge directly above and in the immediate surroundings of the sensor. Depending on where the charge is located, the effective detection range of an EFM varies from a few km to perhaps as much as 20 km. Field changes on the order of a fraction of a second are due to the overall rearrangement of the thundercloud charge distribution produced by a lightning flash, and slower field changes are due to cloud electrification and rearrangement of space charge in the atmosphere. Numerous studies (e.g. Krider, 1989) have taken advantage of the faster field changes to estimate the charge moment changes associated with lightning.

When a cloud first begins to exhibit charge separation nearby or directly above an EFM, there is typically a reversal of the electrostatic field polarity and an increase in the magnitude of the field. Krehbiel (1986) shows an example of the time series of electrostatic field measured directly underneath an essentially stationary small thunderstorm. The polarity change and increase in magnitude is obviously quite useful as a warning of the threat of lightning, given that charge separation has to precede lightning. However, in not all cases does the field reverse polarity at a particular EFM site as a storm develops (Murphy 1996), and the exact magnitude reached by the field depends strongly on the distance between the EFM and the cloud charge regions. Thus, an automated algorithm with a fixed threshold for the field magnitude may or may not pick up all storms.

EFMs may also be used in the case where a mature thunderstorm moves toward the AOC from elsewhere. By far, this represents the vast majority of cases, about 89% according to the analysis described in the appendix. However, it should be noted that almost any lightning detection system has a greater effective

*Corresponding author: Martin Murphy, Vaisala Inc., 2705 E. Medina Rd., Tucson AZ 85706
martin.murphy@vaisala.com

detection range than an EFM, so we expect that a lightning detection system will outperform EFMs for developed storms that move into the AOC from elsewhere. The value of EFMs, therefore, is expected to occur mainly in the 11% or so of cases when a cloud first develops overhead.

In addition to detecting the effects of charge separation in thunderclouds, EFMs also detect a variety of other signals not associated with thunderstorms. These include blowing sand or dust, blowing snow, charge separation in non-lightning producing showers, charge separated when raindrops splash on or near the instrument (depending on the instrument's configuration), and charged aerosols (for example, sea spray near beaches due to breaking waves). See Chalmers (1967), chapters 5-6, for a detailed discussion of these effects. This wide variety of signals can lead to false alarms when EFMs are used for lightning warnings, but the amount of such false alarms will depend greatly on the field threshold used in an automated system as well as the frequency, duration, and intensity of such events.

2. Background

To our knowledge, little work has appeared in the literature describing the performance of EFMs in automated lightning warning systems. Rison and Chapman (1988) described a network of three EFMs at the White Sands Missile Range. The automated algorithm was set up to enable a red light and siren whenever any of the EFMs recorded a field over 1.5 kV/m and keep the warning going until 15 minutes after the field at all 3 sites was below that value. They reported false alarms due to dust storms, but they indicated that in all of their thunderstorm cases (sample size not given), the warning was in effect at least 5 minutes before lightning occurred on site. Hoeft and Wakefield (1992) analyzed a substantial set of cases (72 appear in their Table 1) to determine whether it was appropriate to continue using the U.S. Navy standard field threshold of 2 kV/m or change to another value. Their study, however, had a significant time correlation problem because of the coarseness of the time information accompanying the EFM strip charts. Their study showed high probability of detection (POD), probably due to the necessarily lenient rules used for time correlation between lightning strikes and EFM-based lightning warnings (a few hours or more). The study also indicated a high false alarm ratio (FAR).

Nicholson and Mulvehill (1990) discussed the network of EFMs at the NASA Kennedy Space Center/Cape Canaveral Air Force Station (KSC/CCAFS). While they did not discuss a specific automated warning algorithm, they did describe the pattern of electric fields observed under typical Florida summer thunderstorms. They also discussed false detections and the beginnings of an artificial intelligence-based approach to identifying thunderstorms automatically. Likewise, Montanyá et al. (2004) described a principal component analysis method for utilizing multiple variables in addition to EFM data for lightning warning. The notion of combining EFM data with other sources of information (particularly lightning detection) is also common to Rison and Chapman (1988) and Hoeft and Wakefield (1992).

3. Motivation for the present study

The foregoing introduction and background make it clear that a more systematic study of the contribution of EFMs to lightning warning systems, with a larger and continuous sample of data, is needed. First, we wish to remedy the situation faced by Hoeft and Wakefield (1992) by utilizing continuously recorded and time-stamped EFM data. We also wish to have a much larger sample of storms than one can infer from the discussion given by Rison and Chapman (1988). Finally, given that EFMs are frequently used in conjunction with CG

lightning detection data in automated warning algorithms, we wish to replicate that same set of circumstances with this analysis. We seek to determine the specific contribution of false detections to the problem, and we also wish to assess the effects of varying the parameters by which the EFM data are used in the algorithm.

4. Data and methods

The EFM data come from the KSC/CCAFS EFM network during the summers of 2004 and 2005, where summer is defined here as June, July, and August. All of the KSC/CCAFS EFMs are continuously digitized at a 50 Hz sampling rate, and the data are made available at http://trmm.ksc.nasa.gov. This satisfies one of our major objectives, data continuity. Although the data from all 31 EFMs are recorded, we selected two of the EFM sites in particular, EFMs 5 and 10, for this analysis because they are 3.8 km apart, a geometry that is fairly similar to a typical airport lightning warning system.

The recorded EFM data are broken down into files of 30 minutes duration. Occasionally, one or more of these files was missing or corrupt in some way. In addition, the raw electric field data contained periodic calibration sequences (not during thunderstorm activity), and occasionally there were periods of a few seconds of bad data within an otherwise good sequence of data. All bad data and calibration sequences were removed automatically as we processed the EFM data. Longer periods of missing or corrupt data were compiled in a list, and after all lightning warning start and stop times were computed by the warning analysis algorithm, we then removed all those that overlapped with a period of missing or corrupt EFM data files.

During a thunderstorm, EFMs detect relatively slow field changes (time scale of tens of seconds to minutes) due to the charge separation processes in the cloud as well as the evolution and eventual dissipation of regions of net charge as the storm decays. In addition, they also detect faster (time scale < 1 sec) changes due to the rearrangement of cloud charge by lightning. Lightning-caused field changes can make the field either rise above or drop below a threshold level used in a warning algorithm. For this reason, the data have to be smoothed to lessen the effects of these rapid field changes (note that they can never be completely eliminated without making the data worthless by over-smoothing). Figure 1 shows a sample of EFM data from one of the KSC/CCAFS sensors. We show the original 50-Hz data and two smoothed versions. In our analysis, all smoothing is done using a running average of a particular number of samples. Figure 1 shows smoothed field records corresponding to a 10-second average and a 60-second average. These are the two "smoothing window" values used in the analysis to follow.

In Vaisala lightning warning systems, EFM data are used together with CG flash data from a lightning detection network. For the present study, the lightning data were taken from the U.S. National Lightning Detection Network (NLDN).

The automated warning algorithm involves many of the same parameters as in our past studies (e.g. Murphy and Holle 2006). Figure 2 shows the geographical configuration including the two EFM sites. There is an inner region called the Area Of Concern (AOC); when a CG flash occurs in this region, it is considered an immediate threat, and the objective is to use additional information to provide advance notice prior to the first CG in the AOC, if possible. A second region, called the Warning Area (WA) surrounds the AOC. As in Murphy and Holle (2006), the AOC extends 10 km outward from the center in each direction, and the WA extends 20 km outward.

A warning is triggered if one of three conditions is met: (1) lightning occurs within the WA and at least one of the field values is above a threshold, (2) both field

values are above a threshold, or (3) lightning occurs within the AOC. If lightning occurs within the AOC first, and neither of the other conditions had been satisfied previously, we consider it a failure to warn. If one of the first two conditions is satisfied prior to the first CG flash in the AOC, we consider it a successful warning and compute the lead time between when the warning started and when the first CG occurred in the AOC. A false alarm is any event for which a warning is triggered by condition (1) or (2) above but no CG flash ever occurs inside the AOC. After the three conditions above are no longer satisfied, the warning is continued for 15 minutes (the "dwell time") before it is terminated. For the electric field threshold, we used two different values, 1 kV/m and 2 kV/m.

We measure the performance of the automated warning algorithm using three principal metrics. All of the three metrics depend on three quantities: (1) the number of warning episodes having at least one CG flash in the AOC, (2) the number of episodes in (1) that were successful (see previous paragraph), and (3) the number of false alarm warning episodes (see previous paragraph). If we give these three quantities the names "CGAOC", "SUC", and "FA", then we can define the following three performance metrics for the warning algorithm:

$$POD = \frac{SUC}{CGAOC}$$

$$FTW = 1 - POD$$

$$FAR = \frac{FA}{FA + SUC}$$

The probability of detection (POD) is simply the ratio of the number of successful warnings to the total number of episodes with a CG in the AOC, and the Failure-To-Warn rate (FTW) gives the fraction of unsuccessful warnings (that is, no advance notice prior to first CG in AOC). The False Alarm Ratio (FAR) is measured using only warning episodes triggered by two EFMs above threshold or by a combination of an EFM above threshold and lightning in the WA. Thus, of all warning episodes having CG lightning in the AOC, only the successful ones can appear in the denominator of FAR. This implies an interesting relationship between POD and FAR. In fact, if a change in either the field threshold or the smoothing window results in a significant drop in the number of successful warnings SUC, it is possible for FAR to rise even if the total number of false alarm episodes, FA, also decreases.

For comparison purposes, we also use a CG lightning-only warning technique, as discussed by Murphy and Holle (2006). In this method, a successful warning occurs when CG lightning in the WA preceded CG lightning in the AOC, and a false alarm occurs when CG lightning occurs in the WA only but not in the AOC during a given episode.

5. Results

In section 4, we mentioned that we used two different smoothing windows for the electric field data, 10 sec and 60 sec, and two different electric field thresholds, 1 kV/m and 2 kV/m. Thus, we have four combinations of parameters related to the EFM data. Obviously the CG lightning data do not change, and we do not alter anything about the configuration of the WA and AOC (see Fig. 2) or the dwell time. Tables 1-4 give the statistics for each of the 6 months of data analyzed (June, July, August of 2004 and 2005) and the summary of all months taken together. Each table corresponds to one of the four combinations of EFM-related parameters just discussed. Finally, Table 5 provides an overall summary of the results. These tables are discussed in the following paragraphs.

Table 1. Summary of warning episodes using an electric field smoothing window of 60 sec and a field threshold of 1 kV/m. Variables "CGAOC", "SUC", and "FA" are defined in section 4. Summary of POD, FTW, and FAR for the entire time period is given in the last row.

month	warnings	CGAOC	SUC	FA
Jun 04	44	29	10	15
Jul 04	30	16	3	14
Aug 04	72	32	11	40
Jun 05	52	11	7	41
Jul 05	26	14	5	12
Aug 05	36	29	8	7
Total	**260**	**131**	**45**	**129**
POD = 0.344	**FTW = 0.656**		**FAR = 0.741**	

Table 2. Summary of warning episodes using an electric field smoothing window of 60 sec and a field threshold of 2 kV/m.

month	warnings	CGAOC	SUC	FA
Jun 04	41	33	4	8
Jul 04	31	20	3	11
Aug 04	57	36	9	21
Jun 05	34	11	4	23
Jul 05	22	15	2	7
Aug 05	44	33	1	11
Total	**228**	**148**	**23**	**81**
POD = 0.155	**FTW = 0.845**		**FAR = 0.779**	

Table 3. Summary of warning episodes using an electric field smoothing window of 10 sec and a field threshold of 1 kV/m.

month	warnings	CGAOC	SUC	FA
Jun 04	39	28	10	11
Jul 04	30	16	3	14
Aug 04	67	32	14	35
Jun 05	53	11	7	43
Jul 05	25	14	6	11
Aug 05	36	29	9	7
Total	**250**	**130**	**49**	**120**
POD = 0.377	**FTW = 0.623**		**FAR = 0.710**	

Table 4. Summary of warning episodes using an electric field smoothing window of 10 sec and a field threshold of 2 kV/m.

month	warnings	CGAOC	SUC	FA
Jun 04	40	33	7	7
Jul 04	26	19	3	7
Aug 04	57	35	9	22
Jun 05	50	14	8	36
Jul 05	22	15	2	7
Aug 05	45	33	4	12
Total	**240**	**149**	**33**	**91**
POD = 0.221	**FTW = 0.779**		**FAR = 0.734**	

Table 5. Comparison of the three performance metrics over the two summers for the four combinations of EFM-related parameters. For comparison, the last row shows the results obtained using a CG lightning-only warning technique.

parameters	POD	FTW	FAR
60 sec/1 kV/m	0.344	0.656	0.741
60 sec/2 kV/m	0.155	0.845	0.779
10 sec/1 kV/m	0.377	0.623	0.710
10 sec/2 kV/m	0.221	0.779	0.734
CG lightning only	0.667	0.333	0.684

The first major result that we draw from the POD, FTW, and FAR statistics presented above is that POD is quite poor (0.15-0.38) and FAR is quite high (0.71-0.78). If we were to rely on CG lightning in the WA to provide warnings and remove the EFMs entirely, the POD and FAR for the same time period would be 0.667 and 0.684, respectively, as shown in the last row of Table 5. Thus it appears that the addition of EFMs hinders the performance of a warning system relative to what can be accomplished using CG lightning data alone, at least in summer thunderstorms in Florida. The higher POD observed when CG lightning in the WA is allowed to trigger warnings is consistent with the idea that most storms approach the AOC from elsewhere and are already producing lightning by the time they arrive.

The POD suffers the most when EFMs are used, regardless of the field threshold or smoothing window, although POD is

obviously higher if the field threshold is lower. We believe that a combination of factors causes this to occur in our study. First, the sizes of the AOC and WA are inconsistent with the effective ranges of the EFMs. Second, the EFM effective range is determined by the environment in which these thunderstorms and measurements occur. In Florida summer thunderstorms, the main negative charge region that is responsible for the field polarity reversal observed at most locations under the cloud is located at a rather high altitude, 7-8 km (e.g. Jacobson and Krider, 1976), and the EFMs are located essentially at sea level. Thus there is a large distance between the cloud charge and the EFMs, and the field often does not get very high before lightning is produced. If the field measurement is made at a higher altitude (e.g. New Mexico; see Krehbiel, 1986), or the cloud charge is at a much lower altitude (e.g. Japan winter storms; see Brook et al. 1982), then the field is much more likely to reach a few kV/m or more prior to the first lightning discharge. The large distance between the EFMs and cloud charge in Florida in summer thus limits the effective ranges of the EFMs. Because of the limited range of the EFMs, it is unlikely that either of the field values can reach our thresholds when a storm is in the WA and is approaching the AOC. This results in a very low POD. We might expect to have higher POD in a different geographic location where the cloud charge and EFMs are closer together.

Because the effective ranges of the EFMs are limited, we have to use low field thresholds in Florida in the summertime even to obtain the low POD values that we have. For this reason, we are also more susceptible to false alarms. In fact, we find that a number of our false alarm events are triggered when the two EFMs go above threshold and no CG flash occurs within the WA. This suggests that we might improve performance by not allowing a warning to be initiated if only the two field values go above threshold without lightning. Table 6 summarizes the percentages of all false alarm episodes that are due to the two EFMs alone, and it shows what the POD and FAR would be if we did not permit the two EFMs by themselves to trigger a warning. We find that we are able to make progress reducing the FAR, but we also reduce the POD even further in the process.

Table 6. Analysis of false alarm events due to having 2 field values above threshold and no CG lightning in the WA. The last two columns show the POD and FAR obtained if we do not allow 2 EFMs to trigger a warning by themselves.

parameters	% of FA due to 2 EFMs	new POD	new FAR
60 sec/ 1 kV/m	50.4	0.267	0.646
60 sec/ 2 kV/m	44.4	0.142	0.682
10 sec/ 1 kV/m	51.6	0.300	0.598
10 sec/ 2 kV/m	47.3	0.208	0.608

6. Conclusions and Future Work

We have analyzed the performance of an automated lightning warning algorithm of the type frequently used at airports, in which warnings are triggered on the basis of a combination of CG lightning data in a Warning Area and electric fields' rising above a threshold. For this analysis, we used continuously recorded EFM data from KSC/CCAFS over two summer seasons. We find that this particular automated algorithm performs poorly relative to an algorithm based on CG lightning data alone. The low POD appears to be due to an interaction between the sizes of our WA and AOC and the environment in which the storms occur. This environment, in which the cloud charge and the EFMs are relatively far apart, limits the effective ranges of the EFMs to an area smaller than the AOC and WA.

There are a few possible ways to address the low POD that we observe in

this analysis. First, we can make the AOC and WA smaller in order to be more consistent with the effective ranges of the EFMs for Florida summer storms. Alternatively, the EFMs could be more widely distributed in space (e.g., within the WA itself as well as within the AOC). Finally, we could alter the criteria, allowing a warning to be triggered any time lightning occurs within the WA. Other alterations to the criteria for initiating a warning may also make it possible to utilize electric field information in the most effective way.

As it stands in this analysis, we use rather low field thresholds to deal with the fact that the cloud charge in Florida summer storms is rather far from the EFMs. The use of low field thresholds leads to rather high FAR values. Data at sites other than KSC/CCAFS are required to determine whether the same algorithm will perform better in an area where the cloud charge and EFMs are closer together and the field threshold can be raised to several kV/m.

Finally, the title and abstract of this paper mention total lightning mapping observations. Our initial efforts in this paper ended up being devoted entirely to the use of EFMs. However, we plan to compare these results with warnings based on total lightning mapping data, and perhaps a combination of both EFMs and total lightning observations. Continuous total lightning mapping observations are available from the KSC/CCAFS LDAR system, and we are obtaining those data for inclusion in this study. In addition, we operate total lightning mapping systems in the Dallas-Fort Worth, Texas, and Tucson, Arizona, regions. During the coming year, we will be making continuous EFM recordings in those two areas so that we can pursue this analysis in areas outside Florida as well.

References

Brook, M., M. Nakano, P. Krehbiel, and T. Takeuti, 1982: The electrical structure of the Hokuriku winter thunderstorms. *J. Geophys. Res.*, **87**, 1207-1215.

Chalmers, J.A., 1967: *Atmospheric Electricity*, New York: Pergamon Press.

Hoeft, R. and C. Wakefield, 1992: Evaluation of the electric field mill as an effective and efficient means of lightning detection. *1992 Intl. Aerospace and Ground Conf. on Lightning and Static Electricity*, Atlantic City, NJ, National Interagency Coordinating Group, pp. 4-1 to 4-13.

Jacobson, E.A. and E.P. Krider, 1976: Electrostatic field changes produced by Florida lightning. *J. Atmos Sci.*, **33**, 103-117.

Krehbiel, P.R., 1986: The electrical structure of thunderstorms, in *The Earth's Electrical Environment*, E.P. Krider *et al.*, eds. Washington, DC: National Academy Press, 263 pp.

Krider, E.P., 1989: Electric field changes and cloud electrical structure. *J. Geophys. Res.*, **94**, 13145-13149

Montanyá, J., J. Bergas, and B. Hermoso, 2004: Electric field measurements at ground level as a basis of lightning hazard warning. *J. Electrostatics*, **60**, 241-246.

Murphy, M.J. and R.L. Holle, 2006: Warnings of cloud-to-ground lightning hazard based on combinations of lightning detection and radar information. *Proceedings, 19th Intl. Lightning Detection Conf.*, Tucson, AZ, Vaisala Inc., CD-ROM.

Murphy, M.J., 1996: *The electrification of Florida thunderstorms*. PhD thesis, Univ. of Arizona, available from University Microfilms Inc.

Nicholson, J.R. and A.M. Mulvehill, 1990: Expert knowledge techniques applied to the analysis of electric field mill data. *16th Conf. on Severe Local Storms/Conf. on*

Atmospheric Electricity, Kananaskis Park, Alberta, Amer. Meteorol. Soc., pp. J36-J39.

Rison, W. and G.P. Chapman, 1988: Lightning protection for high explosives and instrumentation using a field mill system. *1988 Intl. Aerospace and Ground Conf. on Lightning and Static Electricity*, Oklahoma City, OK, Natl. Oceanic and Atmospheric Administration, pp. 289-293.

Appendix:

Analysis of the fraction of storms that develop directly overhead

Recently, we attempted to answer the question of how frequently storms develop directly overhead, as opposed to moving in from elsewhere. This analysis was not originally designed to accompany this particular study, and therefore, the region of interest was the Dallas-Fort Worth metropolitan area, where we operate regional total lightning mapping networks. Obviously, in the future the analysis can be repeated for other locations, such as KSC/CCAFS. This appendix describes the method and results obtained from the analysis.

We used nearly 4 years of continuous NLDN data for this analysis (specifically, 1 Jan. 2003 to 28 Sept. 2006). The specific region of interest consisted of nine grid squares with sizes of 0.1º latitude by 0.1º longitude. The full latitude-longitude region was from 32.8 to 33.1º latitude and -97.1 to -96.8º longitude. In the time dimension, the data were broken into five-minute intervals.

The analysis was concentrated on the central grid square. In that square, we searched the NLDN data for what we defined as a "storm start": any five-minute period with at least 2 flashes in the central grid square, before which there were at least 30 minutes with no lightning in the central square. For each storm start, we then searched the eight neighboring grid squares for any lightning activity in the previous five-minute interval, and if we found any, we considered that storm to be one that moved in from the surrounding area. Any "storm start" that had no lightning in any surrounding grid square in the previous five-minute interval was considered a storm that developed overhead.

Over the period of analysis, there were 87 storm starts in the central grid square. Of these, 10 were considered storms that developed overhead. This represents 11.5% of the storm starts. Thus we find that 88.5% of storms move in from elsewhere and 11.5% develop overhead, according to this analysis.

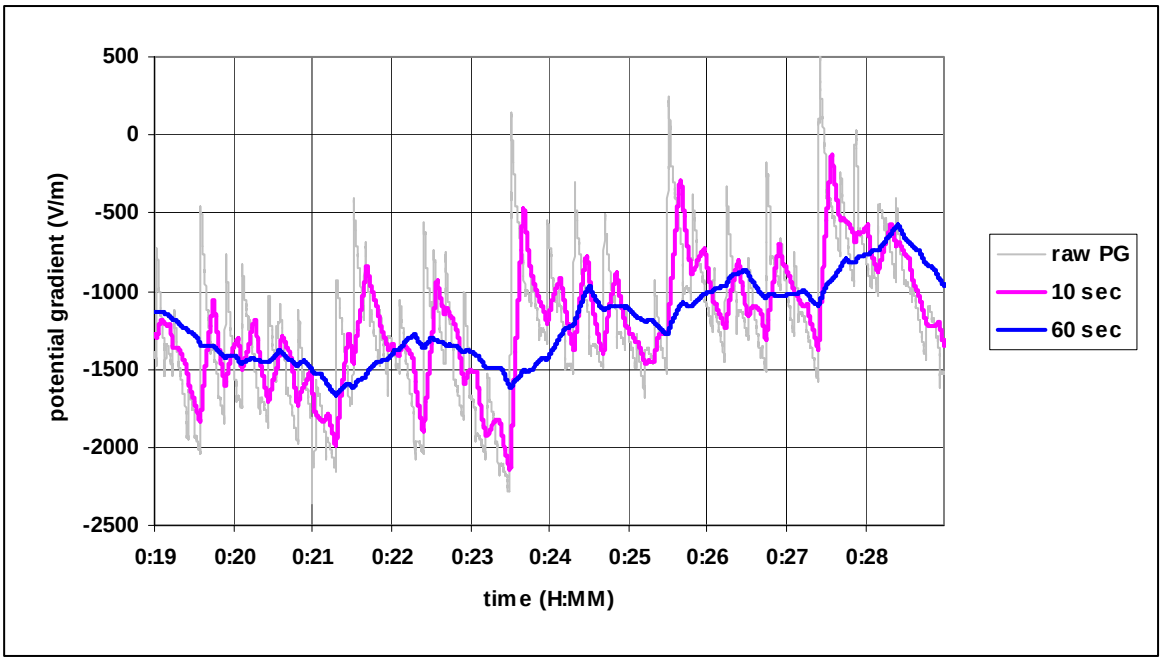

Fig. 1. Raw (50-Hz) potential gradient measurement during a 10-minute period of a thunderstorm (light gray) together with 10-sec and 60-sec smoothed values of the same time period.

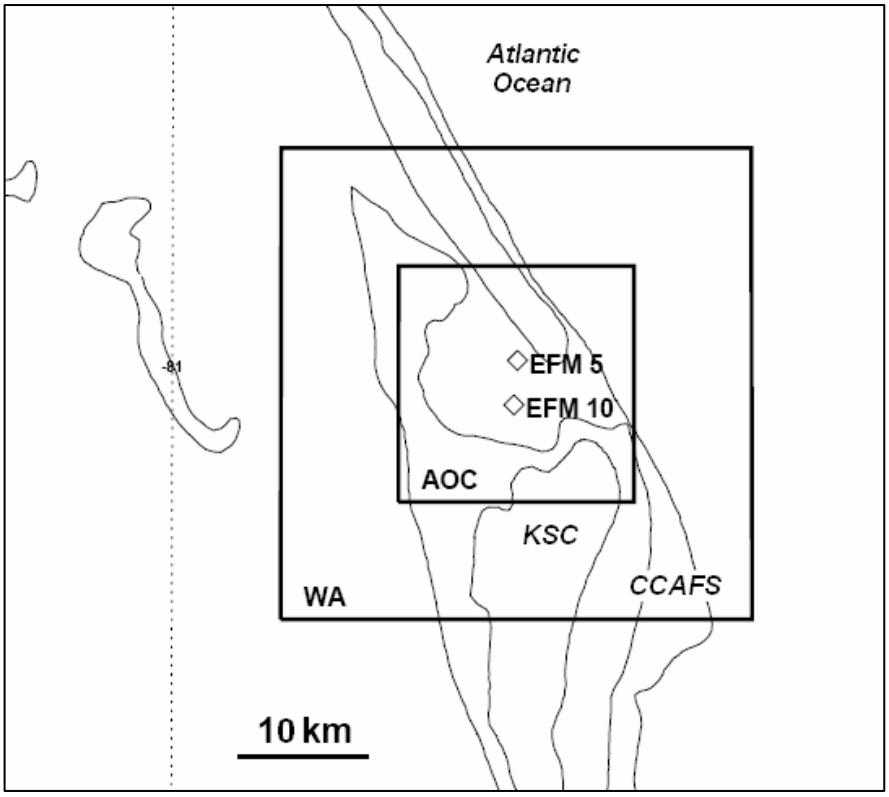

Fig. 2. Warning regions and EFM configuration for this study.